Title

CRISPR/Cas14 and G-Quadruplex DNAzyme-Driven Biosensor for Paper-Based Colorimetric Detection of African Swine Fever Virus.

Journal

ACS Sensors, 9(5)

Authors

Zhao, Xue

He, Yawen

Shao, Shengjie

et al.

Publication Date

2024-05-24

DOI

10.1021/acssensors.4c00090

Peer reviewed

HHS Public Access

Author manuscript

ACS Sens. Author manuscript; available in PMC 2024 July 01.

Published in final edited form as:

ACS Sens. 2024 May 24; 9(5): 2413–2420. doi:10.1021/acssensors.4c00090.

CRISPR/Cas14 and G-Quadruplex DNAzyme-Driven Biosensor for Paper-Based Colorimetric Detection of African Swine Fever Virus

Xue Zhao,
Department of Biological Systems Engineering, Virginia Tech, Blacksburg, Virginia 24061, United States

Yawen He,
Department of Biological Systems Engineering, Virginia Tech, Blacksburg, Virginia 24061, United States

Shengjie Shao,
Department of Biological Systems Engineering, Virginia Tech, Blacksburg, Virginia 24061, United States

Qiaoqiao Ci,
Department of Biological Systems Engineering, Virginia Tech, Blacksburg, Virginia 24061, United States

Lin Chen,
School of Chemistry, Chemical Engineering and Biotechnology, Nanyang Technological University, Singapore 637459, Singapore

Xiaonan Lu,
Department of Food Science and Agricultural Chemistry, Faculty of Agricultural and Environmental Sciences, McGill University, Quebec H9X 3 V9, Canada

Qian Liu,
Institute of Parasitology, McGill University, Quebec H9X 3 V9, Canada

Juhong Chen
Department of Biological Systems Engineering, Virginia Tech, Blacksburg, Virginia 24061, United States; Department of Bioengineering, University of California, Riverside, California 92521, United States

Abstract

Corresponding Author Juhong Chen – *Department of Biological Systems Engineering, Virginia Tech, Blacksburg, Virginia 24061, United States; Department of Bioengineering, University of California, Riverside, California 92521, United States;* jchen@ucr.edu.

Supporting Information

The Supporting Information is available free of charge at https://pubs.acs.org/doi/10.1021/acssensors.4c00090.
Sequences of G-quadruplex (G4), probes, and sgRNA used in this study; sequences of wild-type and mutated ASFV dsDNA and primers used in this study; cost analysis of the CRISPR/Cas14a-G4 biosensor; comparison of the cost by different CRISPR/Cas-based biosensors; electropherogram of G-quadruplex (G4); and optimization of the molar ratio of Cas14a to sgRNA in the CRISPR/Cas14a cleaving system (PDF)

The authors declare no competing financial interest.

The highly contagious nature and 100% fatality rate contribute to the ongoing and expanding impact of the African swine fever virus (ASFV), causing significant economic losses worldwide. Herein, we developed a cascaded colorimetric detection using the combination of a CRISPR/Cas14a system, G-quadruplex DNAzyme, and microfluidic paper-based analytical device. This CRISPR/Cas14a-G4 biosensor could detect ASFV as low as 5 copies/μL and differentiate the wild-type and mutated ASFV DNA with 2-nt difference. Moreover, this approach was employed to detect ASFV in porcine plasma. A broad linear detection range was observed, and the limit of detection in spiked porcine plasma was calculated to be as low as 42–85 copies/μL. Our results indicate that the developed paper platform exhibits the advantages of high sensitivity, excellent specificity, and low cost, making it promising for clinical applications in the field of DNA disease detection and suitable for popularization in low-resourced areas.

Graphical Abstract

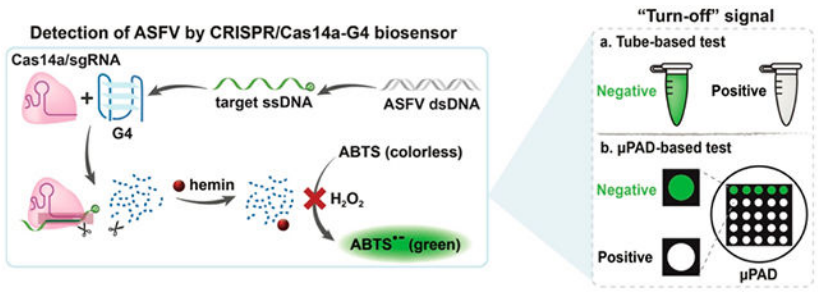

Keywords

African swine fever virus; CRISPR; Cas14; G-quadruplex; pathogen detection; microfluidic paper-based analytical device

African swine fever is a deadly hemorrhagic disease affecting domestic pigs and wild boars caused by African swine fever virus (ASFV). Characterized by its high contagion and 100% fatality rate, ASFV has emerged in 45 countries worldwide since 2020, resulting in over 2,000,000 reported death cases according to the WHO Situation Report as of 2022.11.21.[1,2] This tick-borne virus exhibits genetic diversity with 22 viral genotypes, and its ability to undergo complex immune escape mechanisms contributes to constant mutation and evasion of host immunity.[3,4] Due to the absence of effective therapies and commercial vaccines, the current control measures involve culling infected herds and enforcing strict quarantine protocols.[5] Consequently, ASFV has inflicted substantial socioeconomic losses on the global swine industry, prompting its designation as a notifiable disease by the World Organization for Animal Health (OIE). Given these challenges, the development of timely, accurate, and rapid detection approaches for ASFV is critical to preventing further spread and minimizing the economic impact.

Presently, the OIE-recommended ASFV detection methods include isolating the virus, measuring antigen through fluorescent antibody tests, and detecting the viral genome using polymerase chain reaction (PCR).[6,7] While virus isolation remains the gold standard, its time-consuming and intricate nature makes it unsuitable for real-time disease monitoring.[6]

Antigen measurement allows for a large-scale testing but lacks sensitivity in detecting early stage infections.[8] Quantitative PCR (qPCR) stands out as a rapid and highly sensitive technique for ASFV detection, demanding minimal sample volumes while providing real-time and high-sensitivity results.[9] Nonetheless, its widespread application is hindered by the need for expensive equipment and trained operators, limiting its utility in resource-limited settings for processing a large number of samples.[10] Isothermal amplification techniques such as recombinase polymerase amplification (RPA) offer advantages in simplicity and rapid DNA amplification at a constant temperature. However, concerns about high false-positive rates and nonspecific DNA amplification hinder their widespread adoption.[11] Such inconvenient requirements and disadvantages may deter them from becoming the optimal identification method. Consequently, there is a pressing need for a specific, sensitive, equipment-free, rapid assay for detecting ASFV in the field.

The CRISPR/Cas (clustered regularly interspaced short palindromic repeats/CRISPR-associated protein) system has offered extensive application in biosensing.[12-15] The activated CRISPR/Cas systems not only possess the capacity to cleave the target DNA (referred to as the *cis*-cleavage) but also exhibit collateral nonspecific catalytic activities, cutting nonspecific DNA (referred to as the *trans*-cleavage).[16] Various CRISPR/Cas systems, including Cas9, Cas12a, and Cas13, have been utilized for nucleic acid detection.[17-19] The recently identified CRISPR/Cas14, a novel class 2 type V system, exhibits a distinctive targeting activity against single-stranded DNA (ssDNA) in a PAM-independent manner.[20] Notably, Cas14 exhibits a *cis*-cleavage of targeted ssDNA, resulting in the indiscriminate cleavage of ssDNA in *trans.*[21] The target-dependent and nonspecific DNase activity of the Cas14 nuclease has been harnessed as a foundation for a DNA detection platform, establishing a high-fidelity and strongly specific detection system.[22] The creation of CRISPR/Cas14-DETECTR, serving as an exceptionally sensitive CRISPR-based detection method, enables the diagnosis of significant ssDNA and dsDNA pathogens. Various methods have been documented for the generation of ssDNA from dsDNA, and one of the commonly used methods involves utilizing exonucleases, such as T7 exonuclease, through the modification of the amplification primers.[23,24] The T7 exonuclease consistently facilitates the 5′ to 3′ removal of nucleotides from the unnecessary antisense strand. Meanwhile, the hydrolytic activity of the T7 exonuclease against the intended strand is selectively hindered by multiple phosphorothioate (PT) linkages at its 5′-end through amplification with a PT-modified forward primer, thereby offering protection toward target ssDNA. Additionally, CRISPR/Cas14-DETECTR functions as a high-fidelity and robust genotyping tool for detecting single nucleotide polymorphisms in DNA, without being restricted by the requirement for a PAM sequence.[25]

The integration of G-quadruplex (G4, formed by guanine-rich sequences in the presence of specific monovalent cations) into biosensors has gained attention due to its unique structure, increased thermodynamic stability, and distinctive ligand binding properties.[26,27] When combined with hemin, the G4 DNAzyme can be constituted, which could catalyze the 2,2′-azino-bis (3-ethylbenzothiazoline-6-sulfonic acid) diammonium salt (ABTS)-H_2O_2 reaction and result in a color change in solution.[28] Based on these characteristics, G4 can be used for both target recognition and signal transduction, which has been further developed as a G4-based biosensor with easy operation and visualization capability. In addition, it

has recently been reported that Cas12a, when activated by crRNA-recognizing dsDNA targets, could trim G4.[29] We assumed that the peroxidase-mimicking activity of the G4 DNAzyme could be diminished after the cleavage of Cas14. Thus, combining the CRISPR/Cas14a system with the G4 signal element may favor the development of highly sensitive colorimetric assays.

In order to mitigate the reliance on advanced equipment and reduce resource requirements, a microfluidic paper-based analytical device (μPAD) was developed for colorimetric assays. Since their introduction in 2008, μPADs have been applied to a variety of fields, including environmental monitoring, disease diagnosis, and food quality surveillance.[30] Novel PADs have successfully circumvented the disadvantages of traditional microfluidic polymer-fabricated devices, addressing the issues such as complex fabrication, the need for additional pumping systems, and environmental concerns.[31,32] Moreover, its capability for straightforward analyte or reagent storage, reduced sample consumption, accelerated reaction times, improved portability, and the potential for concurrent detection of multiple analytes and qualitative analyses render this system pertinent for diagnostic and bioanalytical applications, especially in resource-limited settings.[33]

In this study, we developed an advanced colorimetric method that integrates CRISPR/Cas14a, G4 DNAzyme, and μPAD for the cost-effective and highly sensitive detection of ASFV genes. In this detection strategy, the ASFV gene (dsDNA) was amplified by PCR, producing amplicons that were digested to generate target ssDNA by the T7 exonuclease. After hybridization with ssDNA, the *trans*-cleavage activity of the CRISPR/Cas14a complex was triggered. Subsequently, the activated CRISPR/Cas14a system indiscriminately cleaved G4 DNAzymes, resulting in the loss of its peroxidase-like activity to catalyze the colorimetric substrates. To further simplify the detection, a μPAD-based colorimetric platform has been developed, allowing for ASFV detection by mixing the CRISPR/Cas14a system with the G4 DNAzyme complex on the hydrophobic wax-based microwell. The results were recorded by a smartphone camera and analyzed using ImageJ software. The feasibility of this detection approach has been verified by detecting ASFV in porcine plasma. According to our current knowledge, this study represents the initial attempt to detect ASFV on the μPAD using the CRISPR/Cas14a-G4 biosensor. This endeavor sets the stage for achieving our ultimate goal of “easy, efficient, and cost-effective virus diagnosis”. Moving forward, we will be dedicated to taking further actions to enhance our biosensor, specifically by actively working to decrease its complexity for improved usability and efficiency.

RESULTS AND DISCUSSION

Detection Principle.

To visually detect ASFV, the target sequence was first amplified by PCR with a PT-modified primer (A*C*T*C*CTATTACGGACGCAACGTAT; Figure 1a). Afterward, the T7 exonuclease reliably catalyzed the 5′ to 3′ removal of nucleotides from dsDNA and selectively acted on the unmodified strand rather than the target ssDNA with a protective PT linkage.[34,35] Figure 1b shows a schematic illustration of the CRISPR/Cas14a-G4 biosensor for colorimetric detection of ASFV. The resultant PT-containing target single-

stranded ASFV products will complement the specially designed sgRNA and activate the *cis*-cleavage activity of the Cas14a nuclease. The activated Cas14a/sgRNA complex will indiscriminately cleave the surrounding G-rich sequence (namely, *trans*-cleavage activity). This further inhibits the peroxidase-like activity, preventing it from catalyzing the colorimetric substrate of ABTS.[36] Conversely, the intact G4 can bind hemin and catalyze the colorimetric substrate, resulting in a green color in the absence of the target DNA. This enables straightforward differentiation of the results via visual inspection, given the distinct color variations between positive and negative samples. The absorbance intensity can be determined by using a microplate reader for further quantification. Figure 1b also presents the workflow of colorimetric ASFV detection on a μPAD. The target ssDNA can be added to the μPAD with a preloaded Cas system and G4. Upon sequential loading of hemin and ABTS, the colorimetric reaction on the μPAD is initiated, while the developed color of ABTS under the catalyzation activity of G4 can be captured using a smartphone and subsequently transferred to ImageJ software for additional pixel analysis.

Characterization of the CRISPR/Cas14a-G4 Biosensor.

To test the feasibility of our proposed detection approach, we first monitored the fluorescence signal from BHQ-FAM G4 reporters to monitor the cleavage of G4 by the CRISPR/Cas14a. The specific G4 DNAzyme with a G-rich sequence was designed based on a previous study.[29] The cleavage was corroborated based on the fluorescence intensity from G4 reporters, as shown in Figure 2a. The Cas14a/sgRNA system exhibits strong cleavage activation toward ssDNA targets, while almost no fluorescence signal output was observed in its absence or under incomplete Cas14a/sgRNA system conditions. Then we used gel electrophoresis to further verify the cleavage of G4 by the CRISPR/Cas14a complex. Figure 2b demonstrates that G4 was fully cleaved by Cas14a/sgRNA in the presence of the target ssDNA activator as no band was displayed in the fifth lane. As a comparison, the controls without the ssDNA activator (the fourth lane) or the complete Cas14a/sgRNA complex (the first and second lanes) displayed a clear band of G4 on the gel.

Moreover, UV–vis absorption spectroscopy of the mixture of ABTS and H_2O_2 was performed under different conditions. As shown in Figure 2c, the activator-free samples with or without the coexistence of Cas14/sgRNA had a specific absorbance peak at 418 nm, which indicates that G4 formed DNAzyme in complex with the cofactor hemin and exhibits a very high catalytic activity toward H_2O_2–ABTS.[29] However, we noticed that the absorbance peak was dramatically decreased to a negligible level when the target ssDNA activator was further added, suggesting the disruption of G4 by activated Cas14a.

Optimization of the Experimental Conditions.

The optimization process involved a systematic investigation of several parameters that could potentially impact the colorimetric assay with the aim of achieving the best analytical performance. This included examining the concentrations of Cas14a, G4, hemin, H_2O_2, and ABTS, as well as the incubation temperature.

First, we optimized the concentration of Cas14a based on the molar ratio of Cas14a protein to sgRNA of 1:1.25, which had been optimized in our preliminary experiment (Figure S2).

As depicted in Figure 3a, it was noted that the disparity in absorbance (ΔAbs, representing the difference in absorbance intensity between the no template control and the positive sample) became increasingly pronounced as the concentrations of Cas14a rose, reaching a zenith at a concentration of 80 nM for Cas14a (100 nM for sgRNA). Excessive Cas14/sgRNA complexes notably reduced the absorbance signal. It may be attributed to the presence of dithiothreitol, a reducing agent incorporated in the storage buffer designed to safeguard the activity of Cas14a, directly scavenging the ABTS-free radicals.[37]

To further improve the naked-eye detectability of the colorimetric signal using the CRISPR/Cas14a-G4 biosensor, we optimized the concentration of G4 ranging from 50 to 600 nM. As observed in Figure 3b, the maximum visual contrast between positive and negative groups was obtained when the concentration of G4 reached 400 nM. More G4 did not increase the absorbance signal as the Cas14a amount was restricted and the cleavage of G4 was incomplete.[29] Therefore, a concentration of 400 nM for G4 was selected as the optimal level for Cas14-based colorimetric detection.

Meanwhile, because the absorbance signal was affected by hemin, H_2O_2, and ABTS, it is necessary to evaluate and optimize the appropriate concentrations of all of these reagents. As shown in Figure 3c-e, we observed that the ΔAbs became more significant with increasing concentrations and reached a plateau when the concentrations of hemin, H_2O_2, and ABTS were above 400 nM, 125 mM, and 4 mM, respectively. Different incubation temperatures were further assessed to modify this CRISPR/Cas14a-G4 biosensor. Our results also showed that G4 showed better binding performance to hemin under 25 °C than that of 37 °C (Figure 3f).[38,39] Thus, the optimal incubation temperature was set at 25 °C for this cascade detection.

Sensitivity of the CRISPR/Cas14a-G4 Biosensor.

Under optimal conditions, we estimated the analytical performance of the CRISPR/Cas14a-G4 biosensor for detecting ASFV in both microcentrifuge tubes and μPADs. To assess the detection sensitivity of the developed assay, 10-fold dilutions of ASFV dsDNA ranging from 0 to 10^{11} copies were employed. The sample underwent PCR amplification, ssDNA preparation, and colorimetric detection using the CRISPR/Cas14a-G4 biosensor in microcentrifuge tubes. As shown in Figure 4a, a good linear relationship was obtained between the absorbance intensity and concentration of ASFV in the range of 10–10^6 copies/μL for the tube-based colorimetric test (R^2 = 0.921). The corresponding detection limit for ASFV as calculated by using the average of the control replicates plus three times the standard deviation was as low as 5 copies/μL.[40]

In addition, we tested the detection sensitivity of the developed CRISPR/Cas14a-G4 biosensor on a μPAD. In the μPAD-based test, the optical intensity of the developed color was obtained. The ASFV dsDNA samples (0–10^{11} copies/μL) were amplified, degraded to ssDNA, and subjected to the subsequent CRISPR/Cas14a-G4 based colorimetric detection on a μPAD. The colorimetric results were recorded by a smartphone camera and analyzed using the ImageJ software. As presented in Figure 4b, a wider linear range (10^2 to 10^{10} copies/μL; R^2 = 0.9366) was achieved between the color intensity (as expressed by the G/R value) and the ASFV dsDNA in the colorimetric μPAD test. The detailed

values within this linear range for both the green and red channels are further plotted separately, as shown in Figure 4c, respectively. As calculated, the detection limit of ASFV for the μPAD-based CRISPR/Cas14a-G4 biosensor was as low as 19 copies/μL. The detection limit of the CRISPR/Cas14a-G4 biosensor was comparable and even better than other diagnosis methods, such as direct loop-mediated isothermal amplification (LAMP) incorporated into Hive-Chip (30 copies/μL),[41] real-time LAMP assay (30 copies/μL),[42] RPA-coupled CRISPR/Cas12a (3.07 copies/μL),[43] and magnetic bead-based DNA capture assisted with qPCR- and RPA-based detection (100 copies/μL).[44] These results suggest that our developed biosensor combining the G4 DNAzyme and the CRISPR/Cas14a system could be a promising tool for ASFV detection. Furthermore, the cost is approximately $1.07 USD/per reaction (Table S3), rendering it an affordable and cost-effective method for the broad detection of ASFV compared to other CRISPR/Cas-based biosensors (Table S4).

Specificity of the CRISPR/Cas14a-G4 Biosensor.

To investigate the ability of the CRISPR/Cas14a-G4 biosensor to specifically detect ASFV, we introduced a series of two-base mutations to the target ASFV.[7] As depicted in Figure 5a, the target sequences complementary to the guide sequences of sgRNA were randomly mutated with a 2 nt mismatch. The perfect-matched wild-type (WT) target and 2-bp mutants were subjected to the CRISPR/Cas14a-G4 biosensor for the cleavage activity of Cas14a toward G4 and subsequent colorimetric reaction mediated by the G4 DNAzyme. A buffer solution devoid of any ssDNA was employed as a negative control.

As shown in the photographs of Figure 5b, the WT ssDNA samples had a strong “turn-off” signal, presenting a visible transparent color. However, all tested 2 nt mutations of ASFV samples exhibited a light green color similar to that of the control group with no template. The absorbance intensity in the presence of WT ASFV was observed as 12.07 and 11.31 times lower than that of the negative control and mutants, respectively. The distinct color changes can be easily identified visually in the photographs. There were also substantial distinctions between WT and ASFV mutants by comparing the absorbance signal strength ($P < 0.05$), indicating the high specificity of Cas14a-based detection for ASFV sequences. The mutation of the ASFV prevents its binding with sgRNA though the sequence of WT and mutants only has 2 nt differences. Without sgRNA binding, the CRISPR/Cas14a-G4 biosensor cannot be activated for the cleavage of G4.

As expected, similar results were observed in the colorimetric μPAD test, favoring the specificity of the CRISPR/Cas14a-G4 biosensor when applied on the μPAD. Specifically, the color changes can be easily identified visually in the photographs as no “turn-off” signal was observed with all mutated ASFV samples and the no template control (Figure 5c). There were also substantial distinctions between WT and ASFV mutants by comparing the pixel intensity ($P < 0.05$). Taken together, these data demonstrated that the CRISPR/Cas14a-G4 biosensor has a good specificity toward ASFV. Our results indicate that this novel Cas14-based detection platform presents high fidelity in targeting ASFV sequence recognition. This positions CRISPR/Cas14a-G4 biosensor as a valuable high-fidelity detection tool for identifying medically important pathogens.[20,45]

Detection of ASFV in Porcine Plasma.

To confirm the functionality of our system and assay with porcine plasma from infected animals, we spiked varying concentrations of ASFV dsDNA and tested the samples using our system.[34] Figure 6a shows the schematic workflow to detect ASFV in porcine plasma. Generally, the spiked porcine plasma samples were amplified with PCR using 5′ PT-primer and digested with the T7 exonuclease to generate single-stranded ASFV DNA. Afterward, the Cas14a/sgRNA complex and G4 were added to activate the *cis*- and *trans*-cleavage activities of the Cas nuclease sequentially. The target ASFV ssDNA was then detected with a CRISPR/Cas14a-G4 biosensor. In the presence of hemin, ABTS containing H_2O_2 as a colorimetric substrate of G4/hemin DNAzyme failed to turn into a light green color if G4 was cleaved by Cas14a. However, there was color change if there was no target or a target with a very low concentration in the spiked samples.

Detection of ASFV in real samples was conducted either in microcentrifuge tubes or on μPAD. The absorbance of the color changes was assessed at a wavelength of 418 nm. As shown in Figure 6b, a linear calibration equation of Abs = 0.119 log C_{ASFV} + 1.1558 (R^2 = 0.9472) was obtained within the range of 10^3–10^8 copies/μL for tube-based detection, along with a limit of detection of 42 ASFV copies/μL. The optical intensity of the developed color on the μPAD was captured and analyzed. As presented in Figure 6c, a robust linear relationship was obtained between the color intensity and concentration of ASFV in the detection range of 10^4–10^{10} copies/μL (R^2 = 0.9409) for μPAD. The corresponding detection limit was calculated as 85 copies/μL. Although pig plasma exhibits a high background and can affect the overall detection sensitivity, our developed method achieved a relatively good sensitivity.[34] It further signifies the applicability and potential of the developed sensor under real clinical conditions. Considering that ASFV DNA is not fully equated to ASFV, we will assess the sensitivity and specificity of our developed platforms in real clinical samples in the future.

CONCLUSIONS

In summary, a novel detection platform for ASFV was established relying on a CRISPR/Cas14a-G4 biosensor. The diagnosis is based on the Cas14a protein to trigger the indiscriminate G4 denaturation after recognizing and *cis*-cleaving the target ASFV, depriving the peroxidase-mimicking activity of the G4 DNAzyme to catalyze the color change of ABTS. On this basis, “signal-off” colorimetric signals can be easily observed with the naked eye and quantifiably analyzed for sensitive detection of ASFV. As a result, the CRISPR/Cas14a-G4 biosensor provides excellent specificity as a two-nucleotide mismatched sequence could be discriminated well from the target DNA and high sensitivity with a limit detection as low as 5 copies/μL. The feasibility of the CRISPR/Cas14a-G4 biosensor in porcine plasma was also well demonstrated, indicating its potential in actual clinical diagnosis.

To further simplify the detection of ASFV and minimize the required resources, μPAD was introduced to facilitate the current CRISPR/Cas14a-G4 biosensor. The overall performance of the μPAD-based sensor was satisfactory, achieving comparable sensitivity and specificity. The pure ASFV and spiked porcine plasma samples can be detected on the μPAD at

low levels of 19 and 85 copies/μL, respectively. By integrating and taking advantage of the CRISPR/Cas14a system, G4 DNAzyme, and μPAD, our colorimetric sensor provides a sensitive, specific, and inexpensive strategy for ASFV detection. While the concept in this study has been demonstrated for detecting the synthetic ASFV target gene, further improvements are necessary to enhance the applicability of our developed CRISPR/Cas14a-G4 biosensor for virus detection, infectious diseases, and potential outbreak diagnosis. Future work will focus on, but not be limited to, utilizing real viruses and clinical samples, in conjunction with prefolded G4 DNAzymes to expedite point-of-care tests.

Supplementary Material

Refer to Web version on PubMed Central for supplementary material.

ACKNOWLEDGMENTS

This work is supported by the NIH National Institute of General Medical Science (R35GM147069). In addition, X.Z. is supported by the Presidential Postdoctoral Fellowship at Virginia Tech.

REFERENCES

(1). Galindo I; Alonso C African Swine Fever Virus: A Review. Viruses 2017, 9 (5), 103. [PubMed: 28489063]

(2). Wang H; Sun Y; Zhou Y; Liu Y; Chen S; Sun W; Zhang Z; Guo J; Yang C; Li Z; et al. Unamplified System for Sensitive and Typing Detection of ASFV by the Cascade Platform That CRISPR-Cas12a Combined with Graphene Field-Effect Transistor. Biosens. Bioelectron 2023, 240, 115637. [PubMed: 37669587]

(3). Zheng Y; Li S; Li S-H; Yu S; Wang Q; Zhang K; Qu L; Sun Y; Bi Y; Tang F; et al. Transcriptome Profiling in Swine Macrophages Infected with African Swine Fever Virus at Single-Cell Resolution. Proc. Natl. Acad. Sci. U.S.A 2022, 119 (19), No. e2201288119. [PubMed: 35507870]

(4). Dixon LK; Islam M; Nash R; Reis AL African Swine Fever Virus Evasion of Host Defences. Virus Res. 2019, 266, 25–33. [PubMed: 30959069]

(5). Wang T; Luo R; Sun Y; Qiu H-J Current Efforts towards Safe and Effective Live Attenuated Vaccines against African Swine Fever: Challenges and Prospects. Infect. Dis. Poverty 2021, 10 (1), 137. [PubMed: 34949228]

(6). Oura CAL; Edwards L; Batten CA Virological Diagnosis of African Swine Fever—Comparative Study of Available Tests. Virus Res. 2013, 173 (1), 150–158. [PubMed: 23131492]

(7). Lu S; Li F; Chen Q; Wu J; Duan J; Lei X; Zhang Y; Zhao D; Bu Z; Yin H Rapid Detection of African Swine Fever Virus Using Cas12a-Based Portable Paper Diagnostics. Cell Discovery 2020, 6 (1), 18. [PubMed: 32284877]

(8). Hutchings GH; Ferris NP Indirect Sandwich ELISA for Antigen Detection of African Swine Fever Virus: Comparison of Polyclonal and Monoclonal Antibodies. J. Virol. Methods 2006, 131 (2), 213–217. [PubMed: 16182385]

(9). Wang A; Jia R; Liu Y; Zhou J; Qi Y; Chen Y; Liu D; Zhao J; Shi H; Zhang J; et al. Development of a Novel Quantitative Real-time PCR Assay with Lyophilized Powder Reagent to Detect African Swine Fever Virus in Blood Samples of Domestic Pigs in China. Transboundary Emerging Dis. 2020, 67 (1), 284–297.

(10). Taylor SC; Nadeau K; Abbasi M; Lachance C; Nguyen M; Fenrich J The Ultimate qPCR Experiment: Producing Publication Quality, Reproducible Data the First Time. Trends Biotechnol. 2019, 37 (7), 761–774. [PubMed: 30654913]

(11). Jang H-I; Rhee K-J; Eom Y-B Antibacterial and Antibiofilm Effects of α-Humulene against Bacteroides Fragilis. Can. J. Microbiol 2020, 66 (6), 389–399. [PubMed: 32073898]

(12). Das T; Anand U; Pal T; Mandal S; Kumar M; Radha; Gopalakrishnan AV; Lastra J. M. P. d. l.; Dey A Exploring the Potential of CRISPR/Cas Genome Editing for Vegetable Crop Improvement: An Overview of Challenges and Approaches. Biotechnol. Bioeng 2023, 120 (5), 1215–1228. [PubMed: 36740587]

(13). Liu Z; Liu J; Yang Z; Zhu L; Zhu Z; Huang H; Jiang L Endogenous CRISPR-Cas Mediated *in situ* Genome Editing: State-of-the-Art and the Road Ahead for Engineering Prokaryotes. Biotechnol. Adv 2023, 68, 108241. [PubMed: 37633620]

(14). Yang Z; Mao S; Wang L; Fu S; Dong Y; Jaffrezic-Renault N; Guo Z CRISPR/Cas and Argonaute-Based Biosensors for Pathogen Detection. ACS Sens. 2023, 8 (10), 3623–3642. [PubMed: 37819690]

(15). Masi A; Antonacci A; Moccia M; Frisulli V; De Felice M; De Falco M; Scognamiglio V CRISPR-Cas Assisted Diagnostics: A Broad Application Biosensing Approach. TrAC Trends Anal. Chem 2023, 162, 117028.

(16). Xu Z; Chen D; Li T; Yan J; Zhu J; He T; Hu R; Li Y; Yang Y; Liu M Microfluidic Space Coding for Multiplexed Nucleic Acid Detection via CRISPR-Cas12a and Recombinase Polymerase Amplification. Nat. Commun 2022, 13 (1), 6480. [PubMed: 36309521]

(17). Hu J; Jiang M; Liu R; Lv Y Label-Free Crispr/Cas9 Assay for Site-Specific Nucleic Acid Detection. Anal. Chem 2019, 91 (16), 10870–10878. [PubMed: 31340642]

(18). Mukama O; Wu J; Li Z; Liang Q; Yi Z; Lu X; Liu Y; Liu Y; Hussain M; Makafe GG; et al. An Ultrasensitive and Specific Point-of-Care CRISPR/Cas12 Based Lateral Flow Biosensor for the Rapid Detection of Nucleic Acids. Biosens. Bioelectron 2020, 159, 112143. [PubMed: 32364943]

(19). Granados-Riveron JT; Aquino-Jarquin G CRISPR/Cas13-Based Approaches for Ultrasensitive and Specific Detection of microRNAs. Cells 2021, 10 (7), 1655. [PubMed: 34359825]

(20). Harrington LB; Burstein D; Chen JS; Paez-Espino D; Ma E; Witte IP; Cofsky JC; Kyrpides NC; Banfield JF; Doudna JA Programmed DNA Destruction by Miniature CRISPR-Cas14 Enzymes. Science 2018, 362 (6416), 839–842. [PubMed: 30337455]

(21). Fang L; Yang L; Han M; Xu H; Ding W; Dong X CRISPR-Cas Technology: A Key Approach for SARS-CoV-2 Detection. Front. Bioeng. Biotechnol 2023, 11, 1158672. [PubMed: 37214290]

(22). Aquino-Jarquin G. CRISPR-Cas14 Is Now Part of the Artillery for Gene Editing and Molecular Diagnostic. Nanomed.: Nanotechnol. Biol. Med 2019, 18, 428–431.

(23). Nikiforov TT; Rendle RB; Kotewicz ML; Rogers YH The Use of Phosphorothioate Primers and Exonuclease Hydrolysis for the Preparation of Single-Stranded PCR Products and Their Detection by Solid-Phase Hybridization. PCR Methods Appl. 1994, 3 (5), 285–291. [PubMed: 8038696]

(24). Svobodová M; Pinto A; Nadal P; O'Sullivan CK Comparison of Different Methods for Generation of Single-Stranded DNA for SELEX Processes. Anal. Bioanal. Chem 2012, 404 (3), 835–842. [PubMed: 22733247]

(25). Savage DF Cas14: Big Advances from Small CRISPR Proteins. Biochemistry 2019, 58 (8), 1024–1025. [PubMed: 30740978]

(26). Yu Y; Li W; Gu X; Yang X; Han Y; Ma Y; Wang Z; Zhang J Inhibition of CRISPR-Cas12a Trans-Cleavage by Lead (II)-Induced G-Quadruplex and Its Analytical Application. Food Chem. 2022, 378, 131802. [PubMed: 35032802]

(27). Otovat F; Bozorgmehr MR; Mahmoudi A; Morsali A Porphyrin-based Ligand Interaction with G-quadruplex: Metal Cation Effects. J. Mol. Recognit 2023, 36 (8), No. e3017. [PubMed: 37025015]

(28). Li W; Li Y; Liu Z; Lin B; Yi H; Xu F; Nie Z; Yao S Insight into G-Quadruplex-Hemin DNAzyme/RNAzyme: Adjacent Adenine as the Intramolecular Species for Remarkable Enhancement of Enzymatic Activity. Nucleic Acids Res. 2016, 44 (15), 7373–7384. [PubMed: 27422869]

(29). Chen X; Wang L; He F; Chen G; Bai L; He K; Zhang F; Xu X Label-Free Colorimetric Method for Detection of *Vibrio Parahaemolyticus* by Trimming the G-Quadruplex DNAzyme with CRISPR/Cas12a. Anal. Chem 2021, 93 (42), 14300–14306. [PubMed: 34645259]

(30). Channon RB; Yang Y; Feibelman KM; Geiss BJ; Dandy DS; Henry CS Development of an Electrochemical Paper-Based Analytical Device for Trace Detection of Virus Particles. Anal. Chem 2018, 90 (12), 7777–7783. [PubMed: 29790331]

(31). Trofimchuk E; Hu Y; Nilghaz A; Hua MZ; Sun S; Lu X Development of Paper-Based Microfluidic Device for the Determination of Nitrite in Meat. Food Chem. 2020, 316, 126396. [PubMed: 32066068]

(32). Huang J-Y; Lin H-T; Chen T-H; Chen C-A; Chang H-T; Chen C-F Signal Amplified Gold Nanoparticles for Cancer Diagnosis on Paper-Based Analytical Devices. ACS Sens. 2018, 3 (1), 174–182. [PubMed: 29282979]

(33). Zhao W; Ali MM; Aguirre SD; Brook MA; Li Y Paper-Based Bioassays Using Gold Nanoparticle Colorimetric Probes. Anal. Chem 2008, 80 (22), 8431–8437. [PubMed: 18847216]

(34). He Q; Yu D; Bao M; Korensky G; Chen J; Shin M; Kim J; Park M; Qin P; Du K High-Throughput and All-Solution Phase African Swine Fever Virus (ASFV) Detection Using CRISPR-Cas12a and Fluorescence Based Point-of-Care System. Biosens. Bioelectron 2020, 154, 112068. [PubMed: 32056963]

(35). Noteborn WEM; Abendstein L; Sharp TH One-Pot Synthesis of Defined-Length ssDNA for Multiscaffold DNA Origami. Bioconjugate Chem. 2021, 32 (1), 94–98.

(36). Zhang Y; Wu Y; Wu Y; Chang Y; Liu M CRISPR-Cas Systems: From Gene Scissors to Programmable Biosensors. TrAC Trends Anal. Chem 2021, 137, 116210.

(37). Bhuyan SK; Wang L; Jinata C; Kinghorn AB; Liu M; He W; Sharma R; Tanner JA Directed Evolution of a G-Quadruplex Peroxidase DNAzyme and Application in Proteomic DNAzyme-Aptamer Proximity Labeling. J. Am. Chem. Soc 2023, 145, 12726–12736. [PubMed: 37276197]

(38). Li J; Yuan T; Yang T; Xu L; Zhang L; Huang L; Cheng W; Ding S DNA-Grafted Hemin with Preferable Catalytic Properties than G-Quadruplex/Hemin for Fluorescent miRNA Biosensing. Sens. Actuators, B 2018, 271, 239–246.

(39). Monte Carlo AR III; Fu J Inactivation Kinetics of G-quadruplex/Hemin Complex and Optimization for More Reliable Catalysis. ChemPlusChem 2022, 87 (7), No. e202200090. [PubMed: 35543203]

(40). Toghi Eshghi S; Li X; Zhang H Targeted Analyte Detection by Standard Addition Improves Detection Limits in Matrix-Assisted Laser Desorption/Ionization Mass Spectrometry. Anal. Chem 2012, 84 (18), 7626–7632. [PubMed: 22877355]

(41). Zhu Y-S; Shao N; Chen J-W; Qi W-B; Li Y; Liu P; Chen Y-J; Bian S-Y; Zhang Y; Tao S-C Multiplex and Visual Detection of African Swine Fever Virus (ASFV) Based on Hive-Chip and Direct Loop-Mediated Isothermal Amplification. Anal. Chim. Acta 2020, 1140, 30–40. [PubMed: 33218487]

(42). Wang D; Yu J; Wang Y; Zhang M; Li P; Liu M; Liu Y Development of a Real-Time Loop-Mediated Isothermal Amplification (LAMP) Assay and Visual LAMP Assay for Detection of African Swine Fever Virus (ASFV). J. Virol. Methods 2020, 276, 113775. [PubMed: 31726114]

(43). Xiong Y; Cao G; Chen X; Yang J; Shi M; Wang Y; Nie F; Huo D; Hou C One-Pot Platform for Rapid Detecting Virus Utilizing Recombinase Polymerase Amplification and CRISPR/Cas12a. Appl. Microbiol. Biotechnol 2022, 106 (12), 4607–4616. [PubMed: 35708748]

(44). Dhandapani G; Nguyen VG; Kim MC; Noh JY; Jang SS; Yoon S-W; Jeong DG; Huynh TML; Le VP; Song D; et al. Magnetic-Bead-Based DNA-Capture-Assisted Real-Time Polymerase Chain Reaction and Recombinase Polymerase Amplification for the Detection of African Swine Fever Virus. Arch. Virol 2023, 168 (1), 21. [PubMed: 36593422]

(45). Padmanaban V; Ranganathan UDK CRISPR-Cas System and Its Use in the Diagnosis of Infectious Diseases. Microbiol. Res 2022, 263, 127100. [PubMed: 35849921]

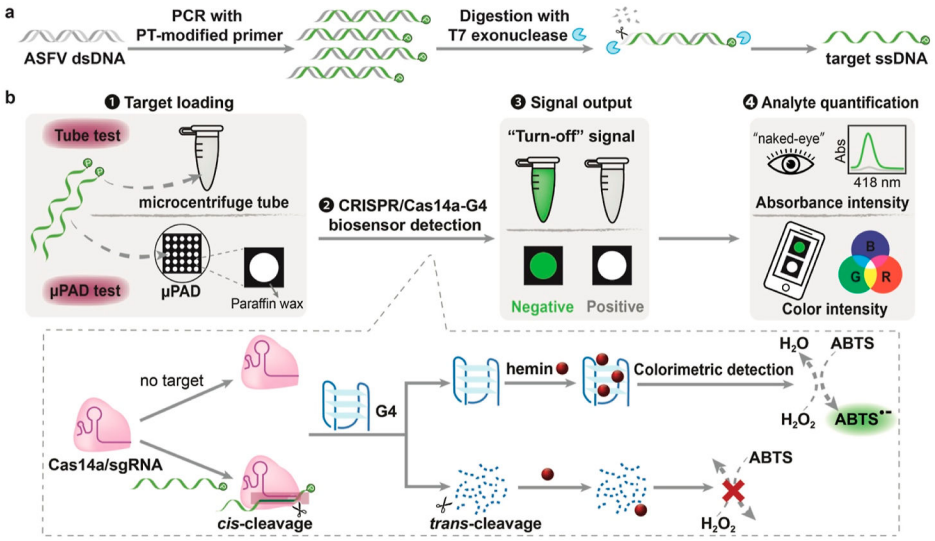

Figure 1.

Schematic illustration of ASFV detection using a CRISPR-Cas14a/G4 biosensor. (a) Schematic illustration of ASFV ssDNA preparation; (b) schematic illustration of target ASFV detection using the CRISPR/Cas14a-G4 biosensor in a microcentrifuge tube or on a *μ*PAD. Notes: PT: phosphorothioate; G4, G-quadruplex.

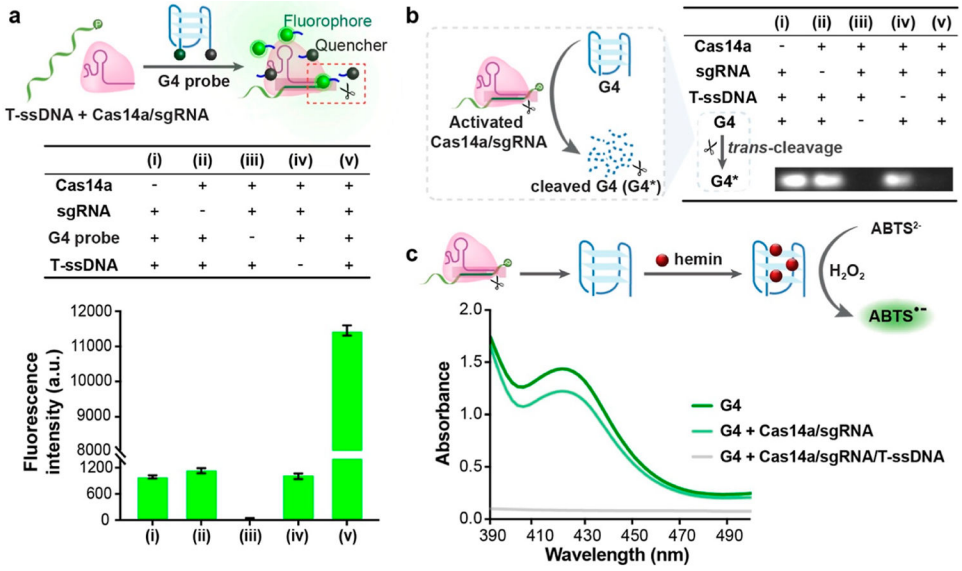

Figure 2.

Characterization of the CRISPR/Cas14a trans-cleaving system toward G4. (a) Fluorescence intensity of BHQ-FAM G4 reporters at 528 nm. (b) Gel electrophoresis results of G4 under different incubation conditions. (c) Absorption spectra of the ABTS and H_2O_2 mixture catalytically oxidized by the G4/hemin complex. Notes: T-ssDNA, target single-stranded DNA; G4, G-quadruplex. Error bars represent the standard deviation between three biological replicates.

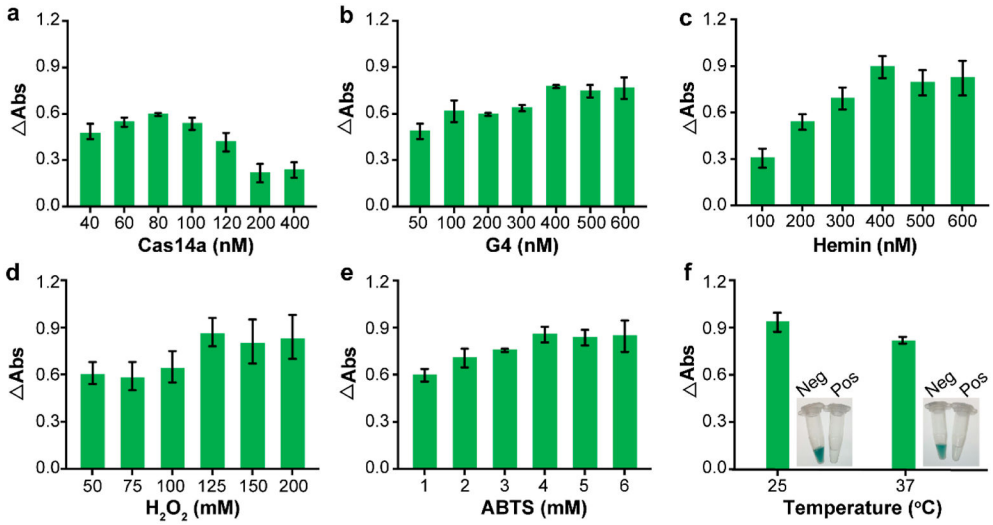

Figure 3.

Optimization of the CRISPR/Cas14a-G4 biosensor. (a) Concentration of Cas14a (nM). (b) Concentration of G4 (nM). (c) Concentration of hemin (nM). (d) Concentration of H_2O_2 (mM). (e) Concentration of ABTS (mM). (f) Incubation temperature (°C) of the G4/hemin complex. Notes: G4, G-quadruplex. Error bars represent the standard deviation between three biological replicates.

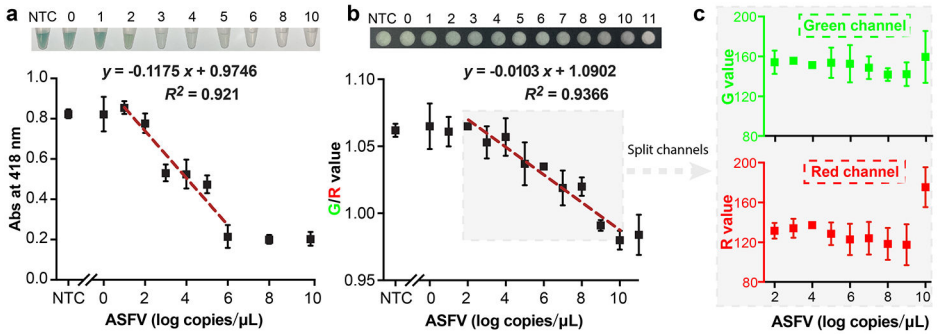

Figure 4.

Sensitivity of the CRISPR/Cas14a-G4 biosensor to detect ASFV. (a) Calibration curve between the absorbance intensity and ASFV concentration. (b) Calibration curve between the color intensity determined by the ImageJ software for the inner section of the reaction chamber intensity and ASFV concentration. (c) Values of red (R) and green (G) channels obtained from the linear range of the original image (b). Notes: NTC, no template control. Error bars represent the standard deviation between three biological replicates.

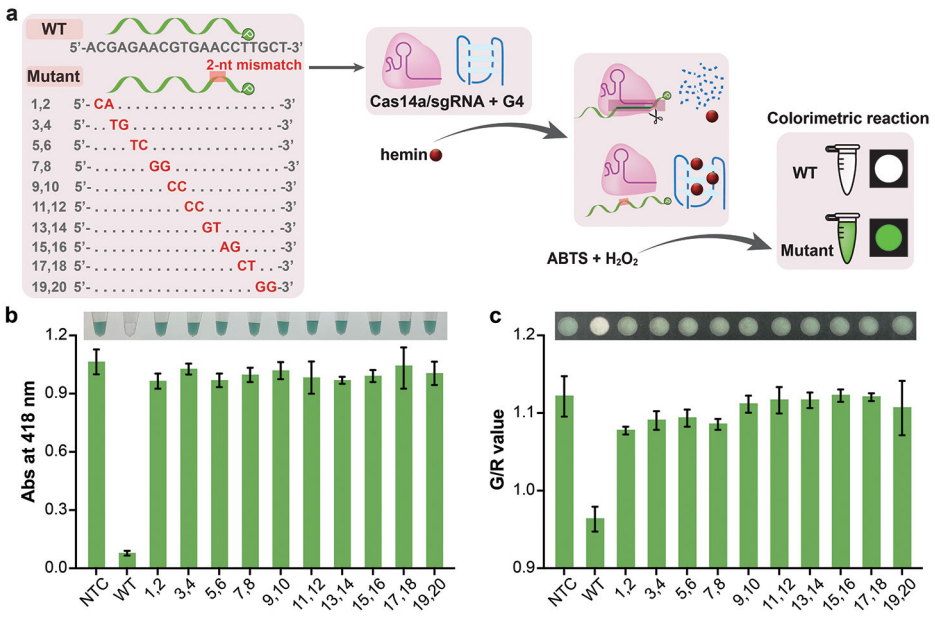

Figure 5.

Specificity of the CRISPR/Cas14a-G4 biosensor. (a) CRISPR/Cas14a-G4 biosensor for the discrimination of sgRNA-targeting perfect match or mutated ASFV dsDNA. (b) Influence of the mutants of the ssDNA target for triggering the colorimetric detection in the microcentrifuge tubes. (c) Influence of the mutants of the ssDNA target for triggering the colorimetric detection on the μPAD. Notes: WT: wild-type; NTC, no template control; G4, G-quadruplex. Error bars represent the standard deviation between three biological replicates.

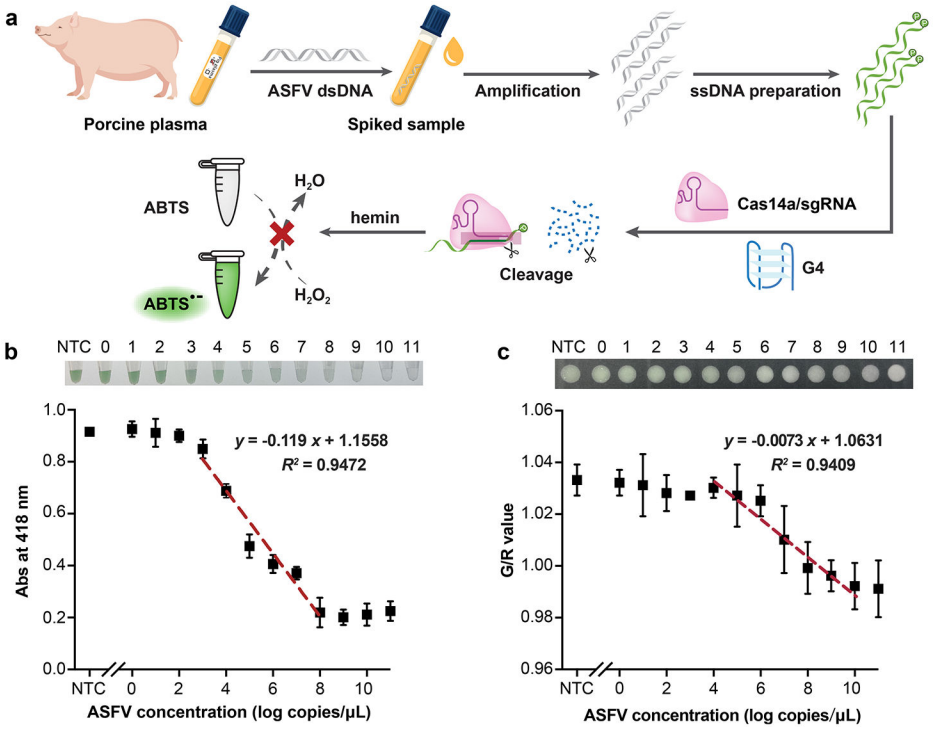

Figure 6.

Application of the CRISPR/Cas14a detection system. (a) Schematic diagram showing the workflow to detect ASFV in porcine plasma. (b) Calibration curve between the absorbance intensity and ASFV concentration. (c) Calibration curve between the color intensity determined by the ImageJ software for the inner section of the reaction chamber and ASFV concentration. Notes: G4, G-quadruplex; NTC, no template control. Error bars represent the standard deviation between three biological replicates.